



## OPEN ACCESS

## EDITED BY

Jian Wu,  
Suzhou Municipal Hospital, China

## REVIEWED BY

Xinyuan Sean Shen,  
University of California, Los Angeles,  
United States  
Zhong Chongning,  
Yanbian University, China

## \*CORRESPONDENCE

Hua Zhu  
✉ hua78314@163.com  
Hongqin Yue  
✉ yuehqy1999@126.com

<sup>†</sup>These authors have contributed equally to this work

RECEIVED 11 March 2025

ACCEPTED 08 April 2025

PUBLISHED 25 April 2025

## CITATION

Yin C, Zhang H, Du J, Zhu Y, Zhu H and Yue H (2025) Artificial intelligence in imaging for liver disease diagnosis. *Front. Med.* 12:1591523.  
doi: 10.3389/fmed.2025.1591523

## COPYRIGHT

© 2025 Yin, Zhang, Du, Zhu, Zhu and Yue. This is an open-access article distributed under the terms of the [Creative Commons Attribution License \(CC BY\)](#). The use, distribution or reproduction in other forums is permitted, provided the original author(s) and the copyright owner(s) are credited and that the original publication in this journal is cited, in accordance with accepted academic practice. No use, distribution or reproduction is permitted which does not comply with these terms.

# Artificial intelligence in imaging for liver disease diagnosis

Chenglong Yin<sup>1,2†</sup>, Huafeng Zhang<sup>3†</sup>, Jin Du<sup>2,4</sup>, Yingling Zhu<sup>2,4</sup>, Hua Zhu<sup>1,2\*</sup> and Hongqin Yue<sup>1,2\*</sup>

<sup>1</sup>Department of Gastroenterology, Affiliated Hospital 6 of Nantong University, Yancheng Third People's Hospital, Yancheng, Jiangsu, China, <sup>2</sup>Affiliated Yancheng Hospital, School of Medicine, Southeast University, Yancheng, Jiangsu, China, <sup>3</sup>Yancheng Ruikang Hospital, Yancheng, Jiangsu, China,

<sup>4</sup>Department of Science and Education, Affiliated Hospital 6 of Nantong University, Yancheng Third People's Hospital, Yancheng, Jiangsu, China

Liver diseases, including hepatitis, non-alcoholic fatty liver disease (NAFLD), cirrhosis, and hepatocellular carcinoma (HCC), remain a major global health concern, with early and accurate diagnosis being essential for effective management. Imaging modalities such as ultrasound (US), computed tomography (CT), and magnetic resonance imaging (MRI) play a crucial role in non-invasive diagnosis, but their sensitivity and diagnostic accuracy can be limited. Recent advancements in artificial intelligence (AI) have improved imaging-based liver disease assessment by enhancing pattern recognition, automating fibrosis and steatosis quantification, and aiding in HCC detection. AI-driven imaging techniques have shown promise in fibrosis staging through US, CT, MRI, and elastography, reducing the reliance on invasive liver biopsy. For liver steatosis, AI-assisted imaging methods have improved sensitivity and grading consistency, while in HCC detection and characterization, AI models have enhanced lesion identification, classification, and risk stratification across imaging modalities. The growing integration of AI into liver imaging is reshaping diagnostic workflows and has the potential to improve accuracy, efficiency, and clinical decision-making. This review provides an overview of AI applications in liver imaging, focusing on their clinical utility and implications for the future of liver disease diagnosis.

## KEYWORDS

liver diseases, artificial intelligence, imaging, diagnosis, clinical applications

## 1 Introduction

Liver diseases, such as hepatitis, non-alcoholic fatty liver disease (NAFLD), cirrhosis, and hepatocellular carcinoma (HCC), continue to pose significant health challenges worldwide (1–3). In 2022, viral hepatitis alone accounts for approximately 1.3 million deaths, making it one of the leading causes of infectious mortality (4–6). NAFLD, affecting nearly a quarter of the global population, is becoming more prevalent due to increasing rates of obesity and metabolic syndrome (7, 8). As these conditions advance, the burden of cirrhosis and HCC continues to rise (9–11), exacerbating healthcare challenges.

The early and precise diagnosis of hepatic disorders is crucial for optimizing clinical outcomes and therapeutic strategies (12). Imaging modalities such as ultrasound (US), computed tomography (CT), and magnetic resonance imaging (MRI) provide non-invasive insights into liver pathology (13–16). However, conventional imaging approaches face inherent limitations, including interobserver variability, reduced sensitivity in early disease stages, and subjective interpretation of subtle pathological changes (17, 18). Artificial intelligence (AI) is transforming medical imaging (19, 20) by enabling automated

image analysis, improving pattern recognition, and enhancing predictive modeling (21–23). AI-driven imaging techniques have demonstrated significant potential in improving the detection, classification, and quantification of liver fibrosis, steatosis, and HCC (24–28). Through the use of deep learning and radiomics, AI enhances diagnostic accuracy and efficiency (29, 30), aiding clinicians in making more informed treatment decisions (Figure 1).

Given the critical role of imaging in liver disease diagnosis, the integration of AI into radiology represents a paradigm shift in diagnostic methodologies. This review explores the integration of AI into liver imaging, emphasizing its applications in fibrosis assessment, steatosis quantification, and HCC detection. Additionally, we discuss the clinical implications of AI-assisted imaging and the challenges associated with its adoption in routine clinical practice.

## 2 Liver fibrosis and cirrhosis

Liver fibrosis, and its advanced stage cirrhosis, are progressive conditions with significant clinical implications, including an increased risk of portal hypertension and HCC. Imaging plays a pivotal role in non-invasive fibrosis staging, reducing reliance on liver biopsy, which is invasive and prone to sampling error (31). AI-driven imaging techniques utilizing US, CT, MRI, and elastography have demonstrated notable promise in improving diagnostic accuracy and fibrosis staging (Table 1).

### 2.1 Ultrasound-based methods

The integration of AI with ultrasonography has demonstrated significant potential for non-invasive fibrosis staging. Lee et al. developed a deep convolutional neural network (DCNN) based on US data from 3,446 patients to stage liver fibrosis, and the high diagnostic accuracy was confirmed through internal and external test sets with 266 and 572 patients, respectively (32). In another study, five US variables were used as input for a neural network, including liver parenchyma, spleen thickness, hepatic vein waveform, hepatic artery pulsatility index, and damping index (33). The network diagnosed liver fibrosis, achieving an area under the curve (AUC) of 0.92.

### 2.2 Computed tomography-based methods

CT imaging provides objective fibrosis assessment, and AI-driven models have further refined its diagnostic potential. Choi et al. used a deep learning system (DLS) to analyze contrast-enhanced CT images of 7,461 patients with histologically confirmed liver fibrosis stages. The DLS showed an overall diagnostic accuracy of 79.4%, with AUCs of 0.95, 0.97, and 0.96 for cirrhosis (F4), advanced fibrosis ( $\geq F3$ ), and significant fibrosis ( $\geq F2$ ) stages, respectively (34). Another study applied a deep learning model based on magnified CT images. The fibrosis scores obtained from deep learning based on CT images ( $F_{DLCT}$  scores) showed significant correlation with the pathological staging of liver fibrosis.

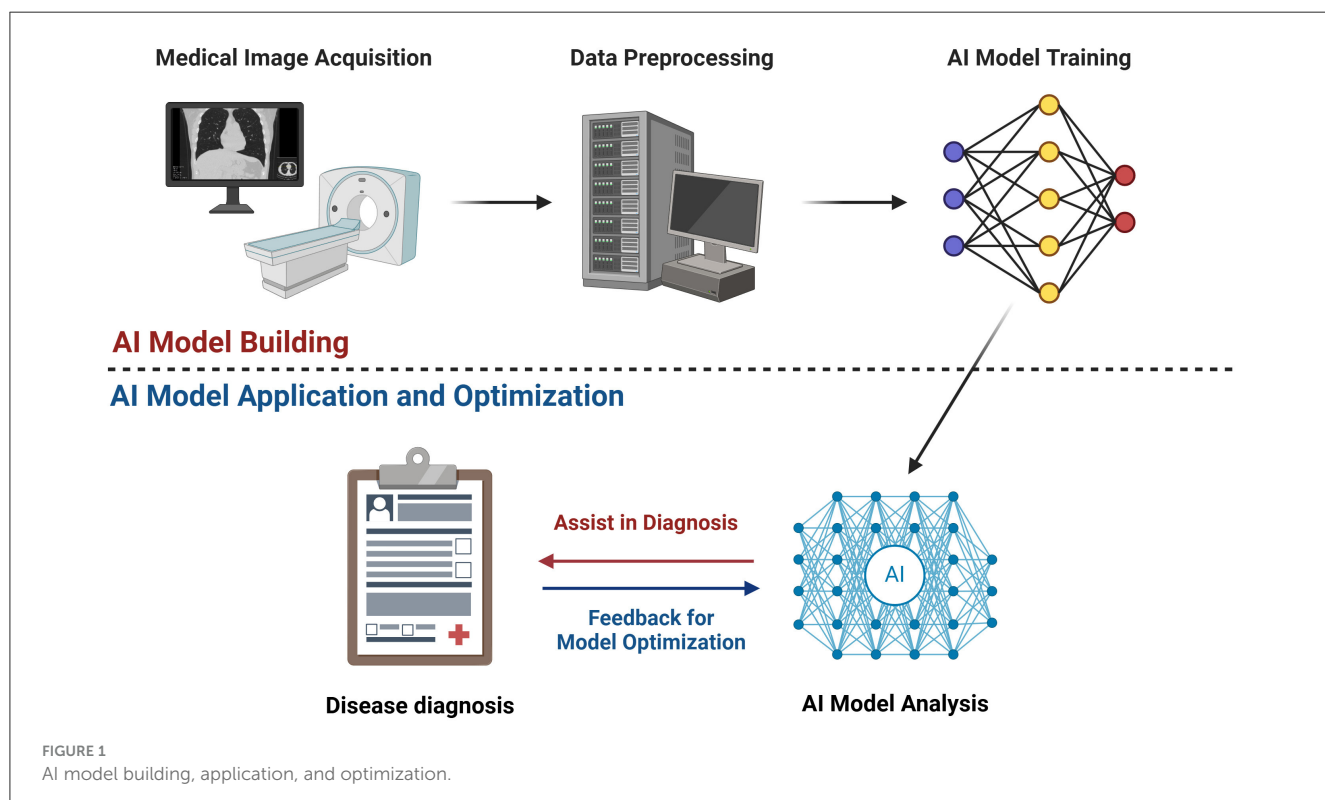


**TABLE 1** The performance of AI in imaging diagnosis of liver fibrosis and cirrhosis.

Imaging technology	Artificial intelligence approaches	Role	Diagnostic performance	References
B-mode US	DCNN	Fibrosis staging	High diagnostic accuracy	(32)
US	NN	Fibrosis diagnosis	AUC = 0.92	(33)
CT	DL	Fibrosis staging	Overall accuracy 79.4%; AUC: F4 = 0.95, $\geq$ F3 = 0.97, $\geq$ F2 = 0.96	(34)
CT	DL	Fibrosis quantification	AUC: F4 = 0.73, $\geq$ F3 = 0.76, $\geq$ F2 = 0.74	(35)
MRI	CNN	Cirrhosis detection	High accuracy for portal hypertension	(36)
MRI	DCNN	Fibrosis staging	AUC: F4 = 0.84, $\geq$ F3 = 0.84, $\geq$ F2 = 0.85	(37)
Elastography	SWE	$\geq$ F2 fibrosis detection	AUC = 0.89 vs. 0.74	(38)
Elastography	DL	Fibrosis staging	Significantly better than conventional liver fibrosis index method	(39)
Elastography	DL	Fibrosis staging	AUC: F4 = 0.97, $\geq$ F3 = 0.98, $\geq$ F2 = 0.85	(40)

Using FDCT scores, the AUCs for predicting stages F4,  $\geq$ F3, and  $\geq$ F2 were 0.73, 0.76, and 0.74, respectively (35).

## 2.3 Magnetic resonance imaging-based methods

MRI-based AI models have advanced fibrosis staging by integrating radiomics and deep learning approaches. Liu et al. developed and validated a radiomics signature, radiomics hepatic venous pressure gradient (rHVPG), as a non-invasive and accurate tool for detecting cirrhosis. This tool can aid in the rapid and non-invasive identification of cirrhosis and portal hypertension and has been extended to MRI (36). In addition, Yasaka et al. conducted a retrospective study to assess the performance of a DCNN model based on gadoxetic acid-enhanced hepatobiliary phase MRI. The fibrosis score obtained through deep learning showed strong correlation with pathological fibrosis staging. The AUCs for diagnosing F4,  $\geq$ F3, and  $\geq$ F2 were 0.84, 0.84, and 0.85, respectively (37).

## 2.4 Elastography-based methods

In addition to US, CT, and MRI, elastography has clear advantages in detecting liver fibrosis and cirrhosis. The automated framework based on shear wave elastography can provide better accuracy in detecting  $\geq$ F2 fibrosis compared to conventional stiffness, with AUCs of 0.89 and 0.74, respectively (38). In another study, 11 image features were extracted from real-time tissue elastography software. Data were processed using four classic classifiers, and it was shown that this method performed significantly better than conventional liver fibrosis index method (39). Wang et al. also developed a deep learning radiomics of elastography (DLRE). As a non-invasive tool, DLRE achieved an AUC of 0.97 for F4, 0.98 for  $\geq$ F3, and 0.85 for  $\geq$ F2 (40).

## 3 Liver steatosis

Diagnosing and grading liver steatosis remain challenging due to the limitations of conventional imaging techniques. While US is widely used, its sensitivity in detecting mild steatosis is limited and highly operator-dependent. CT provides objective liver fat quantification, but exposes patients to ionizing radiation, making it suboptimal for routine screening. The integration of AI with these modalities has significantly improved liver fat quantification, enhancing diagnostic consistency and reducing reliance on invasive liver biopsy (Table 2).

### 3.1 Ultrasound-based methods

AI-enhanced US techniques have shown improved sensitivity in detecting and quantifying liver fat content. Kuppili et al. demonstrated the potential of the extreme learning machine model in stratifying the risk of fatty liver from liver US images, outperforming traditional methods such as support vector machines (SVM) and improving diagnostic speed by 40% (41). Similarly, Byra et al. introduced a DCNN method for evaluating NAFLD (42). In a study, a multi-view ensemble model was shown to perform more accurately than single-view models in assessing liver fat (43). Constantinescu et al. contributed to the field by applying two convolutional neural network (CNN) models for steatosis detection, with Inception-v3 achieving an impressive AUC of 0.93 (44). Kim et al. further combined the VGG19 CNN with multi-view US images, demonstrating that deep learning could replace MRI in detecting fatty liver and estimating fat fraction (45). Another study found deep learning algorithms utilizing radiofrequency US data demonstrated 96% diagnostic accuracy in diagnosing NAFLD, with fat fraction estimations highly correlated to MRI-derived proton density fat fraction (46).

The rapid advancements in AI have also elevated the diagnostic capabilities of US in determining the severity of liver steatosis. Destrempe et al. combined quantitative US with

**TABLE 2** The performance of AI in imaging diagnosis of liver steatosis.

Imaging technology	Artificial intelligence approaches	Role	Diagnostic performance	References
US	ELM	Fatty liver risk stratification	40% faster than SVM	(41)
US	DCNN	NAFLD evaluation	Outperformed traditional methods	(42)
US	MEL	Fat content assessment	Superior to single-view models	(43)
US	CNN	Steatosis detection	AUC = 0.93	(44)
US	CNN + MEL	Fat fraction estimation	Comparable to MRI	(45)
US	DL	NAFLD diagnosis	96% accuracy; high correlation with MRI-PDFF	(46)
US	DL	Steatosis severity	Enhance the classification of liver steatosis	(47)
US	DL	Steatosis severity	Outperformed SVM	(48)
US	DL	Steatosis grading	High classification accuracy	(50)
US	CNN	Classify fatty liver images	AUC = 0.9999	(49)
US	DL	Steatosis grading	AUC: mild = 0.85, moderate = 0.91, severe = 0.93	(51)
US	DL	Steatosis diagnosis	99.91% diagnostic accuracy	(52)
CT	DL	Steatosis grading	93.33% diagnostic accuracy	(53)
CT	DL	NAFLD severity	Outstanding diagnostic performance	(54)
CT	DL	Automated fat quantification	Effective for asymptomatic populations	(55)
CT	NLP	Multi-modal report analysis	>90% recall/accuracy	(56)

shear wave elastography and a random forest model, enhancing the classification of liver steatosis (47). Further studies have demonstrated the superiority of random forest classifiers over SVM in assessing liver steatosis severity (48). Zamani et al. introduced a neural network-based model that achieved a remarkable AUC of 0.9999 in classifying fatty liver images (49). Furthermore, the ResNet-50 v2 model exhibited high classification accuracy for varying levels of liver steatosis (50), while Li et al. employed a deep learning algorithm to quantitatively score liver steatosis with AUCs of 0.85, 0.91, and 0.93 for mild, moderate, and severe grades, respectively (51). Rhyou et al. developed a fully automated model that achieved 99.91% diagnostic accuracy (52). A computer-aided diagnosis (CAD) system achieved a classification accuracy of 93.33% for steatosis grading (53). Cao et al. demonstrated outstanding diagnostic performance of deep learning in US for evaluating the severity of NAFLD (54).

### 3.2 Computed tomography-based methods

The application of AI in conjunction with CT holds significant promise for advancing the diagnosis of liver steatosis. Graffy et al. leveraged deep learning algorithms to automatically assess the CT values of the liver, offering an effective and non-invasive method for evaluating fatty liver in asymptomatic populations undergoing routine screening (55). Similarly, Redmond et al. applied natural language processing to develop an algorithm capable of accurately identifying fatty liver disease, achieving over 90% recall and

accuracy across US, CT, and MRI reports (56). Furthermore, an automated liver attenuation regions of interest-based method has been introduced, showing excellent performance in detecting NAFLD on CT scans (57).

## 4 Hepatocellular carcinoma

The application of AI in HCC imaging has led to notable advancements in lesion detection, classification, and risk stratification. Traditional imaging methods often struggle to distinguish malignant from benign hepatic lesions, particularly in early-stage HCC or atypical presentations. AI-driven approaches have improved diagnostic precision, reduced interobserver variability, and enabled automated risk assessment across US, CT, and MRI (Table 3).

### 4.1 Ultrasound-based methods

AI-based approaches have been developed to enhance the performance of US imaging, particularly in lesion classification, risk stratification, and preoperative assessment. Recent studies have demonstrated the effectiveness of deep learning models in focal liver lesion (FLLs) classification. A neural network ensemble-based CAD model achieved a classification accuracy of 95% (58). Similarly, Bharti et al. developed an ensemble classifier-based model that improved liver disease staging accuracy to 96.6% (59), while Schmauch et al. introduced a supervised deep learning model

**TABLE 3** The performance of AI in imaging diagnosis of hepatocellular carcinoma.

Imaging technology	Artificial intelligence approaches	Role	Diagnostic performance	References
US	NN	FLL classification	95% accuracy	(58)
US	DL	Disease staging	96.6% accuracy	(59)
US	DCNN	FLL classification	Mean AUC = 0.935/0.916	(60)
US	CNN	HCC vs. cirrhotic parenchyma	Outperformed ML models	(61)
US	DCNN	Benign vs. malignant lesions	AUC = 0.924	(62)
US	Multiple kernel learning	FLL classification	Classification accuracy of 90.41%	(67)
US	CEUS + SVM	Atypical HCC vs. FNH	Effective differentiation	(68)
US	CEUS	Preoperative grading	Superior AUC	(69)
CT	CNN	Lesion detection/classification	93.4% recall; 82.5% binary accuracy	(70)
CT	DL	HCC vs. other malignancies	AUC = 0.92	(71)
CT	CNN	Tumor detection	98.3% classification accuracy and 78% tumor detection rate	(72)
CT	CNN+FCN+SSD	Tumor detection	100% detection accuracy	(73)
CT	CNN + SVM	HCC vs. ICC	88% accuracy	(74)
CT	DL	Tumor detection	98.39%–100% detection accuracy	(75)
CT	CNN	Tumor segmentation	Dice = 80.06%; Precision = 82.67%	(78)
CT	FCN	Segmentation (multi-phase CT)	Volume overlap error: 15.6%→ 8.1%	(79)
CT	DL	Segmentation	85% false-positive reduction; Dice = 69%	(80)
CT	DL	Differentiate HCC from other FLLs	Diagnostic accuracy with safety considerations	(83)
CT	CNN	Recurrence monitoring	Detection rate: 72%→ 86%	(84)
MRI	DL	Lesion classification	77% overall accuracy	(85)
MRI	3D CNN	Lesion classification	83% accuracy	(88)
MRI	CNN	LI-RADS grading	90% accuracy; AUC = 0.95	(91)
MRI	DL	HCC differentiation	AUC = 0.999	(92)
MRI	CNN	Automated HCC delineation	Demonstrated feasibility	(93)
MRI	3D CNN	Atypical HCC classification	Overall accuracy = 87.3%; AUC = 0.912	(94)

that achieved mean AUC values of 0.935 and 0.916, respectively (60). Notably, a CNN model using US images has outperformed conventional machine learning models in distinguishing HCC from cirrhotic parenchyma (61). Additionally, for distinguishing between benign and malignant liver lesions, a DCNN model based on US images achieved an AUC of 0.924, surpassing the diagnostic accuracy of experienced radiologists (62).

Ulrasomics, which integrates radiomic feature extraction with machine learning algorithms, has shown promise in differentiating primary and metastatic liver tumors. Logistic regression classifier leveraging ultrasomic features have demonstrated superior performance compared to conventional imaging methods (63). Furthermore, ulrasomics combined with clinical

data has significantly improved the accuracy of preoperative pathological grading of HCC (64) and enhanced non-invasive differentiation between HCC and intrahepatic cholangiocarcinoma (ICC) (65).

Contrast-enhanced ultrasound (CEUS) has also benefited from AI-based approaches. A machine learning-based CAD system demonstrated enhanced diagnostic accuracy for FLL classification (66). Guo et al. employed deep canonical correlation analysis combined with multiple kernel learning in three-phase CEUS imaging, achieving a classification accuracy of 90.41% (67). Huang et al. developed a SVM-based CAD model capable of effectively distinguishing atypical HCC from focal nodular hyperplasia (68). Furthermore, incorporating ultrasound

radiomics and clinical data in multi-phase CEUS imaging has further improved preoperative pathological grading of HCC, achieving superior AUC values compared to single-modality models (69).

## 4.2 Computed tomography-based methods

AI-based CT models have been developed to enhance lesion detection, classification, pathological grading, segmentation, and imaging protocol optimization. A hierarchical CNN framework achieved an average lesion detection accuracy of 82.8%, with a recall of 93.4% and an F1-score of 87.8%, demonstrating robust lesion identification. Additionally, its binary and six-class classification accuracies reached 82.5% and 73.4%, surpassing other neural networks and performing comparably to intermediate-level radiologists (70). In lesion classification, deep learning models analyzing dynamic contrast-enhanced CT images reported an AUC of 0.92 for distinguishing HCC from other malignant liver tumors (71). A CNN-based CAD system achieved a 98.3% classification accuracy and a tumor detection rate of 78%, underscoring AI's potential as a radiological diagnostic aid (72). Further advancements leveraging multiphase CT imaging include models integrating Hounsfield Unit density variations from four-phase CT scans with Faster R-CNN, R-FCN, and SSD networks, achieving a tumor detection accuracy of 100% and lesion classification accuracy of 95.1% (73). Additionally, Ponnoprat et al. combined CNN and SVM classifiers for distinguishing HCC from ICC, achieving an accuracy of 88% (74). Ensemble models integrating multiple classifiers have also been effective, with detection accuracies ranging from 98.39% to 100% and classification accuracies between 76.38% and 87.01%, surpassing individual classifier performances (75).

Beyond lesion classification, AI has been applied to non-invasive tumor grading, aiding in risk stratification. A study analyzing 13,920 quantitative imaging features extracted from three-phase CT scans developed a predictive model that achieved AUCs of 0.70 and 0.66 in discovery and validation cohorts, respectively, aiding in the identification of high-risk HCC patients (76). Another radiomics-based machine learning approach improved the model's AUC to 0.8014 when incorporating radiomic features, reinforcing AI's role in assessing tumor aggressiveness (77).

AI has also contributed significantly to automated tumor segmentation, a crucial step for treatment planning and response assessment. CNN-based segmentation models have outperformed conventional methods, with a Dice coefficient of 80.06%, precision of 82.67%, and recall of 84.34% (78). Another study proposed a multi-channel fully convolutional network that integrated multi-phase contrast-enhanced CT images, achieving a volume overlap error of  $15.6 \pm 4.3\%$  on the 3Dircadb dataset, which further decreased to  $8.1 \pm 4.5\%$  on the JDRD dataset, demonstrating enhanced accuracy and robustness (79). To further optimize segmentation, approaches incorporating voxel- and object-level models have significantly reduced false positives by 85%, achieving Dice coefficients of up to 69%, comparable to manual segmentation (80). Furthermore, adversarial training strategies have been implemented to refine segmentation models, yielding Dice

coefficients of 68.4% while improving multiple segmentation metrics, including ASD, MSD, VOE, and RVD (81). The Successive Encoder-Decoder framework has further refined segmentation workflows, demonstrating Dice coefficients of 92% for liver segmentation and 75% for tumor prediction, emphasizing its clinical applicability (82).

AI has also been leveraged for CT imaging protocol optimization and recurrence monitoring, ensuring effective diagnosis while minimizing radiation exposure. Shi et al. compared three-phase and four-phase DCE-CT protocols for differentiating HCC from other FLLs, and they found that excluding the non-contrast phase did not significantly impact diagnostic performance, while substantially reducing radiation exposure, highlighting AI's role in balancing diagnostic accuracy with safety considerations (83). AI-assisted recurrence monitoring has also demonstrated significant improvements, with a CNN-based classifier integrating baseline and follow-up CT scans increasing new tumor detection rates from 72% to 86%, emphasizing AI's potential in long-term HCC surveillance (84).

## 4.3 Magnetic resonance imaging-based methods

AI applications in MRI have focused on lesion classification, automated detection, pathological grading, and segmentation. In HCC classification, deep learning models leveraging multi-sequence MRI have demonstrated high diagnostic accuracy. A study integrating dynamic contrast-enhanced MRI and T2-weighted images with clinical risk factors developed an automated system that achieved an overall classification accuracy of 0.77 for five common liver lesions (85). CNN-based models trained on large MRI datasets have outperformed radiologists, achieving an accuracy of 92% in lesion classification (86). Further improvements were seen when AI models incorporated additional MRI features. Oyama et al. employed texture analysis and topological data analysis on T1-weighted MRI, achieving an accuracy of 92% in distinguishing HCC from metastatic lesions (87). Trivizakis et al. leveraged 3D CNN to analyze diffusion weighted MRI, achieving an accuracy of 83% and outperforming conventional 2D CNN models, reinforcing the benefits of 3D volumetric feature extraction in liver lesion classification (88).

In automated HCC detection, a fine-tuned CNN model applied to hepatobiliary phase MRI achieved a sensitivity of 87% and specificity of 93%, underscoring its potential in early tumor detection (89). Zhen et al. developed multiple CNN-based models incorporating contrast-enhanced MRI, non-contrast MRI, and clinical data. Even when using non-contrast MRI alone, the model achieved an AUC of 0.946, which further improved to 0.985 when combined with clinical data, yielding a diagnostic concordance of 91.9%, demonstrating AI's ability to optimize non-invasive HCC assessment (90).

AI has also contributed significantly to lesion grading and segmentation, providing a means for automated Liver Imaging Reporting and Data System (LI-RADS) classification and tumor delineation. An AlexNet CNN model applied to multi-phase contrast-enhanced MRI for classifying LI-RADS grading achieved

an accuracy of 90% and an AUC of 0.95, demonstrating performance comparable to expert radiologists (91). Liang et al. developed MRI-based radiomics models using random forest to differentiate hepatic epithelioid angiomyolipoma, HCC, and focal nodular hyperplasia, with an AUC of 0.999 for radiomics alone and 0.971 for an integrated model incorporating clinical features, surpassing conventional diagnostic methods (92). In addition, Bousabarah et al. introduced a CNN-based model trained on multiphasic contrast-enhanced MRI, demonstrating automated HCC detection and delineation (93).

Furthermore, advances in 3D CNN architectures have further improved the classification of atypical HCC. A study using multi-sequence MRI to differentiate typical and atypical HCC from non-HCC lesions reported an overall accuracy of 87.3%, with HCC classification sensitivity/specificity of 92.7%/82.0%, and non-HCC classification sensitivity/specificity of 82.0%/92.7%, achieving an AUC of 0.912 (94).

## 5 Conclusions

AI-driven imaging has significantly improved the detection, classification, and quantification of liver diseases, including

fibrosis, steatosis, and HCC (Figure 2). By enhancing the diagnostic accuracy of US, CT, MRI, and elastography, AI has reduced observer variability and the need for invasive biopsies, offering a transformative approach to liver disease assessment.

However, challenges remain in standardizing imaging protocols, ensuring the generalizability of AI models across diverse populations and healthcare settings, and improving interpretability. Many AI models rely on institution-specific datasets, limiting their broader applicability. In the future, anonymized datasets across ethnicities, scanners, and disease etiologies should be established and used to validate these AI models. Researchers can also develop adaptive AI frameworks which can dynamically adjust to local imaging protocols or population characteristics. Besides, we can align AI validation with FDA/CE guidelines for medical devices. Additionally, the “black-box” nature of deep learning algorithms hinders clinical trust, necessitating the development of more explainable AI frameworks and rigorous validation through multicenter trials.

Although AI models can assist in the diagnosis of liver diseases to some extent, they cannot fully replace liver biopsy, particularly for fibrosis and steatosis, as liver biopsy

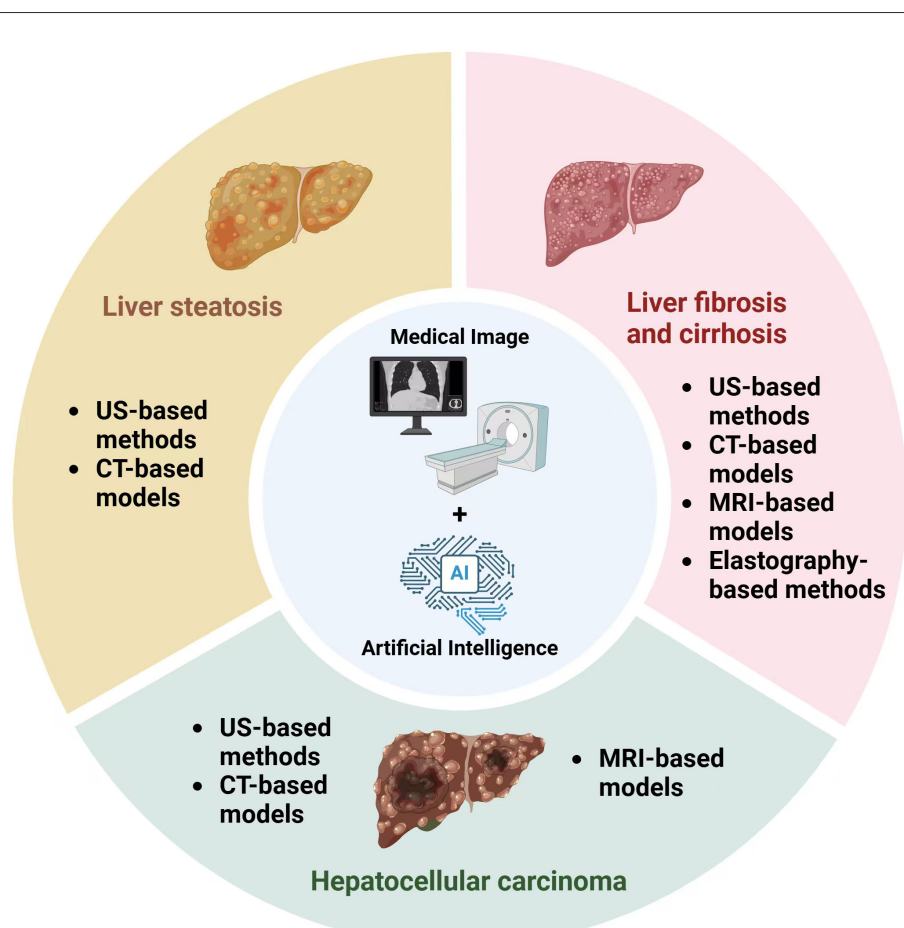


FIGURE 2

Application of AI image models in the diagnosis of fibrosis assessment, steatosis quantification, and hepatocellular carcinoma detection.

remains the gold standard for diagnosing liver fibrosis and steatosis. While AI models for fibrosis staging and steatosis quantification have achieved sensitivities >85% and specificities >90%, they still fall short of biopsy in early-stage disease (F0-F1 fibrosis or <5% steatosis). In such cases, biopsy remains indispensable.

Besides, practical challenges such as computational resource requirements, radiologist acceptance, and regulatory approvals must also be addressed to facilitate integration into clinical workflows. For example, AI tools may require specialized hardware for real-time analysis, and their adoption depends on demonstrating cost-effectiveness and alignment with existing diagnostic pathways. Collaborative efforts between clinicians, data scientists, and policymakers are essential to overcome these barriers.

Despite these limitations, AI holds great promise for revolutionizing liver disease diagnostics. Emerging techniques, such as multi-modal AI integration, are poised to further advance the field. The combination of imaging data with clinical, genomic, and laboratory biomarkers will enhance diagnostic accuracy. For instance, we can couple radiomics features from MRI/CT with serum biomarkers or genetic risk scores, which may improve stratification of high-risk patients. Such multi-modal approaches will address the limitations of single-modality AI by capturing complementary biological insights. Additionally, integrating AI with real-time electronic health records (EHR) may enable dynamic risk prediction models. Future efforts should focus on enhancing model robustness, integrating AI with EHR and multi-omics data, and fostering interdisciplinary collaboration between clinicians, data scientists, and policymakers. With continued innovation, AI can bridge critical gaps in liver disease management, ultimately improving patient outcomes on a global scale.

## References

- Mak L-Y, Liu K, Chirapongsathorn S, Yew KC, Tamaki N, Rajaram RB, et al. Liver diseases and hepatocellular carcinoma in the Asia-Pacific region: burden, trends, challenges and future directions. *Nat Rev Gastroenterol Hepatol.* (2024) 21:834–51. doi: 10.1038/s41575-024-00967-4
- Wu X-N, Xue F, Zhang N, Zhang W, Hou J-J, Lv Y, et al. Global burden of liver cirrhosis and other chronic liver diseases caused by specific etiologies from 1990 to 2019. *BMC Public Health.* (2024) 24:363. doi: 10.1186/s12889-024-17948-6
- Dubey MK., Ahmed K, Dubey S, Pandey DK. Liver diseases: genetic factors, current challenges, and future directions. In: *Computational Intelligence for Genomics Data*. Elsevier (2025). p. 113–121. doi: 10.1016/B978-0-443-30080-6.00021-3
- Organization WH. *Global Hepatitis Report 2024: Action for Access in Low-and Middle-Income Countries*. Geneva: World Health Organization. (2024).
- Huang L, Chen X, Wang Z. Total burden of hepatitis B and C attributed to injecting drug use in 204 countries and territories from 1990 to 2021: analyses based on the Global Burden of Disease Study 2021. *Int J Infect Dis.* (2025) 150:107293. doi: 10.1016/j.ijid.2024.107293
- Suchiita A, Gupta N, Nandi K, Sonkar S, Chandra L. Harmony within: unravelling the microbiome-immune system symbiosis for health. *Adv Gut Microb Res.* (2025) 2025:9927379. doi: 10.1155/agm/9927379
- Gan C, Yuan Y, Shen H, Gao J, Kong X, Che Z, et al. Liver diseases: epidemiology, causes, trends and predictions. *Signal Transd Targeted Ther.* (2025) 10:33. doi: 10.1038/s41392-024-02072-z
- Sookoian S, Pirola CJ, Sanyal AJ. MASLD as a non-communicable disease. *Nat Rev Gastroenterol Hepatol.* (2025) 22:148–9. doi: 10.1038/s41575-025-01039-x
- Asrani SK, Devarbhavi H, Eaton J, Kamath PS. Burden of liver diseases in the world. *J Hepatol.* (2019) 70:151–71. doi: 10.1016/j.jhep.2018.09.014
- Sayiner M, Golabi P, Younossi ZM. Disease burden of hepatocellular carcinoma: a global perspective. *Dig Dis Sci.* (2019) 64:910–7. doi: 10.1007/s10620-019-05537-2
- Tao Z, Zhu H, Zhang J, Huang Z, Xiang Z, Hong T. Recent advances of eosinophils and its correlated diseases. *Front Public Health.* (2022) 10:954721. doi: 10.3389/fpubh.2022.954721
- Wazir H, Abid M, Essani B, Saeed H, Khan MA, Nasrullah F, et al. Diagnosis and treatment of liver disease: current trends and future directions. *Cureus.* (2023) 15:e49920. doi: 10.7759/cureus.49920
- Lăpădat A, Jianu I, Ungureanu B, Florescu L, Gheonea D, Sovaila S, et al. Non-invasive imaging techniques in assessing non-alcoholic fatty liver disease: a current status of available methods. *J Med Life.* (2017) 10:19. doi: 10.25122/jml-2017-0019
- Jiang C, Cai Y-Q, Yang J-J, Ma C-Y, Chen J-X, Huang L, et al. Radiomics in the diagnosis and treatment of hepatocellular carcinoma. *Hepatobiliary Pancreatic Dis Int.* (2023) 22:346–51. doi: 10.1016/j.hbpd.2023.03.010
- Huang W, Peng Y, Kang L. Advancements of non-invasive imaging technologies for the diagnosis and staging of liver fibrosis: Present and future. *View.* (2024) 5:20240010. doi: 10.1002/VIW.20240010
- Butt A, Bach H. Nanomedicine and clinical diagnostics part I: applications in conventional imaging (MRI, X-ray/CT, and ultrasound). *Nanomedicine.* (2025) 20:167–82. doi: 10.1080/17435889.2024.2439776
- Oei EH, van Tiel J, Robinson WH, Gold GE. Quantitative radiologic imaging techniques for articular cartilage composition: toward early diagnosis and development

## Author contributions

CY: Writing – original draft. HZha: Writing – original draft. JD: Writing – original draft. YZ: Writing – original draft. HZhu: Writing – review & editing. HY: Writing – review & editing.

## Funding

The author(s) declare that no financial support was received for the research and/or publication of this article.

## Conflict of interest

The authors declare that the research was conducted in the absence of any commercial or financial relationships that could be construed as a potential conflict of interest.

## Generative AI statement

The author(s) declare that no Gen AI was used in the creation of this manuscript.

## Publisher's note

All claims expressed in this article are solely those of the authors and do not necessarily represent those of their affiliated organizations, or those of the publisher, the editors and the reviewers. Any product that may be evaluated in this article, or claim that may be made by its manufacturer, is not guaranteed or endorsed by the publisher.

- of disease-modifying therapeutics for osteoarthritis. *Arthr Care Res.* (2014) 66:1129–41. doi: 10.1002/acr.22316
18. Chakraborty DP. *Observer Performance Methods for Diagnostic Imaging: Foundations, Modeling, and Applications with r-Based Examples*. London: CRC Press. (2017). doi: 10.1201/9781351228190
  19. Santos MK, Ferreira JR, Wada DT, Tenório APM, Nogueira-Barbosa MH, Marques PM, et al. Artificial intelligence, machine learning, computer-aided diagnosis, and radiomics: advances in imaging towards to precision medicine. *Radiol Brasil.* (2019) 52:387–96. doi: 10.1590/0100-3984.2019.0049
  20. Pinto-Coelho L. How artificial intelligence is shaping medical imaging technology: a survey of innovations and applications. *Bioengineering.* (2023) 10:1435. doi: 10.3390/bioengineering10121435
  21. Barragán-Montero A, Javaid U, Valdés G, Nguyen D, Desbordes P, Macq B, et al. Artificial intelligence and machine learning for medical imaging: a technology review. *Phys Medica.* (2021) 83:242–56. doi: 10.1016/j.ejmp.2021.04.016
  22. Kalita AJ, Boruah A, Das T, Mazumder N, Jaiswal SK, Zhuo GY, et al. Artificial intelligence in diagnostic medical image processing for advanced healthcare applications. In: *Biomedical Imaging: Advances in Artificial Intelligence and Machine Learning*. Springer. (2024). p. 1–61. doi: 10.1007/978-981-97-5345-1\_1
  23. Jiang L, Zuo H, Wang XJ, Chen C. Current applications and future perspectives of artificial intelligence in valvular heart disease. *J Transl Internal Med.* (2025) 13:7–9. doi: 10.1515/jtim-2025-0003
  24. Wang Y, Wu J, Xu J, Lin S. Clinical significance of high expression of stanniocalcin-2 in hepatocellular carcinoma. *Biosci Rep.* (2019) 39:BSR20182057. doi: 10.1042/BSR20182057
  25. Dana J, Venkatasamy A, Saviano A, Lupberger J, Hoshida Y, Vilgrain V, et al. Conventional and artificial intelligence-based imaging for biomarker discovery in chronic liver disease. *Hepatol Int.* (2022) 16:509–22. doi: 10.1007/s12072-022-10303-0
  26. Yuan J, Li J, Gao C, Jiang C, Xiang Z, Wu J. Immunotherapies catering to the unmet medical need of cold colorectal cancer. *Front Immunol.* (2022) 13:1022190. doi: 10.3389/fimmu.2022.1022190
  27. Lu F, Meng Y, Song X, Li X, Liu Z, Gu C, et al. Artificial intelligence in liver diseases: recent advances. *Adv Ther.* (2024) 41:967–90. doi: 10.1007/s12325-024-02781-5
  28. Zhang P, Gao C, Huang Y, Chen X, Pan Z, Wang L, et al. Artificial intelligence in liver imaging: methods and applications. *Hepatol Int.* (2024) 18:422–34. doi: 10.1007/s12072-023-10630-w
  29. Khalifa M, Albadawy M, AI. in diagnostic imaging: revolutionising accuracy and efficiency. *Comput Methods Progr Biomed Update.* (2024) 5:100146. doi: 10.1016/j.cmpcup.2024.100146
  30. Maniaci A, Lavalle S, Gagliano C, Lentini M, Masiello E, Parisi F, et al. The integration of radiomics and artificial intelligence in modern medicine. *Life.* (2024) 14:1248. doi: 10.3390/life14101248
  31. Sterling RK, Duarte-Rojo A, Patel K, Asrani SK, Alsawas M, Dranoff JA, et al. AASLD Practice Guideline on imaging-based noninvasive liver disease assessment of hepatic fibrosis and steatosis. *Hepatology.* (2025) 81:672–724. doi: 10.1097/HEP.0000000000000843
  32. Lee JH, Joo I, Kang TW, Paik YH, Sinn DH, Ha SY, et al. Deep learning with ultrasonography: automated classification of liver fibrosis using a deep convolutional neural network. *Eur Radiol.* (2020) 30:1264–73. doi: 10.1007/s00330-019-06407-1
  33. Zhang L, Li Q, Duan Y, Yan G, Yang Y, Yang R. Artificial neural network aided non-invasive grading evaluation of hepatic fibrosis by duplex ultrasonography. *BMC Med Inform Decis Mak.* (2012) 12:1–6. doi: 10.1186/1472-6947-12-55
  34. Choi KJ, Jang JK, Lee SS, Sung YS, Shim WH, Kim HS, et al. Development and validation of a deep learning system for staging liver fibrosis by using contrast agent-enhanced CT images in the liver. *Radiology.* (2018) 289:688–97. doi: 10.1148/radiol.2018180763
  35. Yasaka K, Akai H, Kunimatsu A, Abe O, Kiryu S. Deep learning for staging liver fibrosis on CT: a pilot study. *Eur Radiol.* (2018) 28:4578–85. doi: 10.1007/s00330-018-5499-7
  36. Liu Y, Ning Z, Örmeci N, An W, Yu Q, Han K, et al. Deep convolutional neural network-aided detection of portal hypertension in patients with cirrhosis. *Clin Gastroenterol Hepatol.* (2020) 18:2998–3007.e2995. doi: 10.1016/j.cgh.2020.03.034
  37. Yasaka K, Akai H, Kunimatsu A, Abe O, Kiryu S. Liver fibrosis: deep convolutional neural network for staging by using gadoteric acid-enhanced hepatobiliary phase MR images. *Radiology.* (2018) 287:146–55. doi: 10.1148/radiol.2017171928
  38. Brattain LJ, Telfer BA, Dhyani M, Grajo JR, Samir AE. Objective liver fibrosis estimation from shear wave elastography. In: *2018 40th Annual International Conference of the IEEE Engineering in Medicine and Biology Society (EMBC)*. IEEE. (2018). p. 1–5. doi: 10.1109/EMBC.2018.8513011
  39. Chen Y, Luo Y, Huang W, Hu D, Zheng R, Cong S, et al. Machine-learning-based classification of real-time tissue elastography for hepatic fibrosis in patients with chronic hepatitis B. *Comput Biol Med.* (2017) 89:18–23. doi: 10.1016/j.combiomed.2017.07.012
  40. Wang K, Lu X, Zhou H, Gao Y, Zheng J, Tong M, et al. Deep learning Radiomics of shear wave elastography significantly improved diagnostic performance for assessing liver fibrosis in chronic hepatitis B: a prospective multicentre study. *Gut.* (2019) 68:729–41. doi: 10.1136/gutjnl-2018-316204
  41. Kuppili V, Biswas M, Sreekumar A, Suri HS, Saba L, Edla DR, et al. Extreme learning machine framework for risk stratification of fatty liver disease using ultrasound tissue characterization. *J Med Syst.* (2017) 41:1–20. doi: 10.1007/s10916-017-0797-1
  42. Byra M, Styczyński G, Szmiigelski C, Kalinowski P, Michałowski Ł, Palusziewicz R, et al. Transfer learning with deep convolutional neural network for liver steatosis assessment in ultrasound images. *Int J Comput Assist Radiol Surg.* (2018) 13:1895–903. doi: 10.1007/s11548-018-1843-2
  43. Byra M, Han A, Boehringer AS, Zhang YN, O'Brien Jr WD, Erdman Jr JW, et al. Liver fat assessment in multiview sonography using transfer learning with convolutional neural networks. *J Ultras Med.* (2022) 41:175–84. doi: 10.1002/jum.15693
  44. Constantinescu EC, Udrășoiu A-L, Udrășoiu SC, Iacob AV, Gruiuonu LG, Gruiuonu G, et al. Transfer learning with pre-trained deep convolutional neural networks for the automatic assessment of liver steatosis in ultrasound images. *Med Ultrason.* (2021) 23:135–9. doi: 10.11152/mu-2746
  45. Kim T, Lee DH, Park E-K, Choi S. Deep learning techniques for fatty liver using multi-view ultrasound images scanned by different scanners: development and validation study. *JMIR Med Inform.* (2021) 9:e30066. doi: 10.2196/30066
  46. Han A, Byra M, Heba E, Andre MP, Erdman Jr JW, Loomba R, et al. Noninvasive diagnosis of nonalcoholic fatty liver disease and quantification of liver fat with radiofrequency ultrasound data using one-dimensional convolutional neural networks. *Radiology.* (2020) 295:342–50. doi: 10.1148/radiol.2020191160
  47. Destrempe F, Gesnik M, Chayer B, Roy-Cardinal M-H, Olivé D, Giard J-M, et al. Quantitative ultrasound, elastography, and machine learning for assessment of steatosis, inflammation, and fibrosis in chronic liver disease. *PLoS ONE.* (2022) 17:e0262291. doi: 10.1371/journal.pone.0262291
  48. Mihailescu DM, Gui V, Toma CI, Popescu A, Sporea I. Computer aided diagnosis method for steatosis rating in ultrasound images using random forests. *Med Ultrason.* (2013) 15:184–90. doi: 10.11152/mu.2013.2066.153.dmm1vg2
  49. Zamani H, Mostaari A, Azadeh P, Ahmadi M. Implementation of combinational deep learning algorithm for non-alcoholic fatty liver classification in ultrasound images. *J Biomed Phys Eng.* (2021) 11:73. doi: 10.31661/jbpe.v0i0.2009-1180
  50. Chou T-H, Yeh H-J, Chang C-C, Tang J-H, Kao W-Y, Su I-C, et al. Deep learning for abdominal ultrasound: a computer-aided diagnostic system for the severity of fatty liver. *J Chinese Med Assoc.* (2021) 84:842–50. doi: 10.1097/JCMA.0000000000000585
  51. Li B, Tai D-I, Yan K, Chen Y-C, Chen C-J, Huang S-F, et al. Accurate and generalizable quantitative scoring of liver steatosis from ultrasound images via scalable deep learning. *World J Gastroenterol.* (2022) 28:2494. doi: 10.3748/wjg.v28.i22.2494
  52. Rhyou S-Y, Yoo J-C. Cascaded deep learning neural network for automated liver steatosis diagnosis using ultrasound images. *Sensors.* (2021) 21:5304. doi: 10.3390/s21165304
  53. Ribeiro RT, Marinho RT, Sanches JM. An ultrasound-based computer-aided diagnosis tool for steatosis detection. *IEEE J Biomed Health Inform.* (2013) 18:1397–403. doi: 10.1109/JBHI.2013.2284785
  54. Cao W, An X, Cong L, Lyu C, Zhou Q, Guo R. Application of deep learning in quantitative analysis of 2-dimensional ultrasound imaging of nonalcoholic fatty liver disease. *J Ultrasound Med.* (2020) 39:51–9. doi: 10.1002/jum.15070
  55. Graffy PM, Sandfort V, Summers RM, Pickhardt PJ. Automated liver fat quantification at nonenhanced abdominal CT for population-based steatosis assessment. *Radiology.* (2019) 293:334–42. doi: 10.1148/radiol.2019190512
  56. Redman JS, Natarajan Y, Hou JK, Wang J, Hanif M, Feng H, et al. Accurate identification of fatty liver disease in data warehouse utilizing natural language processing. *Dig Dis Sci.* (2017) 62:2713–8. doi: 10.1007/s10620-017-4721-9
  57. Huo Y, Terry JG, Wang J, Nair S, Lasko TA, Freedman BI, et al. Fully automatic liver attenuation estimation combining CNN segmentation and morphological operations. *Med Phys.* (2019) 46:3508–19. doi: 10.1002/mp.13675
  58. Virmani J, Kumar V, Kalra N, Khandelwal N. Neural network ensemble based CAD system for focal liver lesions from B-mode ultrasound. *J Digit Imaging.* (2014) 27:520–37. doi: 10.1007/s10278-014-9685-0
  59. Bharti P, Mittal D, Ananthasivan R. Preliminary study of chronic liver classification on ultrasound images using an ensemble model. *Ultrasound Imaging.* (2018) 40:357–79. doi: 10.1177/0161734618787447
  60. Schmauch B, Herent P, Jehanno P, Dehaene O, Saillard C, Aubé C, et al. Diagnosis of focal liver lesions from ultrasound using deep learning. *Diagn Interv Imaging.* (2019) 100:227–33. doi: 10.1016/j.diii.2019.02.009
  61. Brehar R, Mitrea D-A, Vancea F, Marita T, Nedevschi S, Lupșor-Platon M, et al. Comparison of deep-learning and conventional machine-learning methods for the automatic recognition of the hepatocellular carcinoma areas from ultrasound images. *Sensors.* (2020) 20:3085. doi: 10.3390/s20113085

62. Yang Q, Wei J, Hao X, Kong D, Yu X, Jiang T, et al. Improving B-mode ultrasound diagnostic performance for focal liver lesions using deep learning: A multicentre study. *EBioMedicine*. (2020) 56:102777. doi: 10.1016/j.ebiom.2020.102777
63. Mao B, Ma J, Duan S, Xia Y, Tao Y, Zhang L. Preoperative classification of primary and metastatic liver cancer via machine learning-based ultrasound radiomics. *Eur Radiol*. (2021) 31:4576–86. doi: 10.1007/s00330-020-07562-6
64. Ren S, Qi Q, Liu S, Duan S, Mao B, Chang Z, et al. Preoperative prediction of pathological grading of hepatocellular carcinoma using machine learning-based ultrasomics: a multicenter study. *Eur J Radiol*. (2021) 143:109891. doi: 10.1016/j.ejrad.2021.109891
65. Ren S, Li Q, Liu S, Qi Q, Duan S, Mao B, et al. Clinical value of machine learning-based ultrasomics in preoperative differentiation between hepatocellular carcinoma and intrahepatic cholangiocarcinoma: a multicenter study. *Front Oncol*. (2021) 11:749137. doi: 10.3389/fonc.2021.749137
66. Ta CN, Kono Y, Eghtedari M, Oh YT, Robbin ML, Barr RG, et al. Focal liver lesions: computer-aided diagnosis by using contrast-enhanced US cine recordings. *Radiology*. (2018) 288:1062–71. doi: 10.1148/radiol.2017170365
67. Guo L-H, Wang D, Qian Y-Y, Zheng X, Zhao C-K, Li X-L, et al. A two-stage multi-view learning framework based computer-aided diagnosis of liver tumors with contrast enhanced ultrasound images. *Clin Hemorheol Microcirc*. (2018) 69:343–54. doi: 10.3233/CH-170275
68. Huang Q, Pan F, Li W, Yuan F, Hu H, Huang J, et al. Differential diagnosis of atypical hepatocellular carcinoma in contrast-enhanced ultrasound using spatio-temporal diagnostic semantics. *IEEE J Biomed Health Inform*. (2020) 24:2860–9. doi: 10.1109/JBHI.2020.2977937
69. Wang W, Wu S-S, Zhang J-C, Xian M-F, Huang H, Li W, et al. Preoperative pathological grading of hepatocellular carcinoma using ultrasomics of contrast-enhanced ultrasound. *Acad Radiol*. (2021) 28:1094–101. doi: 10.1016/j.acra.2020.05.033
70. Zhou J, Wang W, Lei B, Ge W, Huang Y, Zhang L, et al. Automatic detection and classification of focal liver lesions based on deep convolutional neural networks: a preliminary study. *Front Oncol*. (2021) 10:581210. doi: 10.3389/fonc.2020.581210
71. Yasaka K, Akai H, Abe O, Kiryu S. Deep learning with convolutional neural network for differentiation of liver masses at dynamic contrast-enhanced CT: a preliminary study. *Radiology*. (2018) 286:887–96. doi: 10.1148/radiol.2017170706
72. Khan AA, Narejo GB. Analysis of abdominal computed tomography images for automatic liver cancer diagnosis using image processing algorithm. *Curr Med Imag*. (2019) 15:972–82. doi: 10.2174/1573405615666190716122040
73. Phan A-C, Cao H-P, Trieu T-N, Phan T-C. Improving liver lesions classification on CT/MRI images based on Hounsfield Units attenuation and deep learning. *Gene Expr Patterns*. (2023) 47:119289. doi: 10.1016/j.gep.2022.119289
74. Ponnoprat D, Inkeaw P, Chaijaruwanich J, Traisathit P, Sripan P, Inmutto N, et al. Classification of hepatocellular carcinoma and intrahepatic cholangiocarcinoma based on multi-phase CT scans. *Med Biol Eng Comput*. (2020) 58:2497–515. doi: 10.1007/s11517-020-02229-2
75. Krishan A, Mittal D. Ensembled liver cancer detection and classification using CT images. *Proc Inst Mech Eng Part H*. (2021) 235:232–44. doi: 10.1177/0954411920971888
76. Mokrane F-Z, Lu L, Vavasseur A, Otal P, Peron J-M, Luk L, et al. Radiomics machine-learning signature for diagnosis of hepatocellular carcinoma in cirrhotic patients with indeterminate liver nodules. *Eur Radiol*. (2020) 30:558–70. doi: 10.1007/s00330-019-06347-w
77. Mao B, Zhang L, Ning P, Ding F, Wu F, Lu G, et al. Preoperative prediction for pathological grade of hepatocellular carcinoma via machine learning-based radiomics. *Eur Radiol*. (2020) 30:6924–32. doi: 10.1007/s00330-020-07056-5
78. Li W, Jia F, Hu Q. Automatic segmentation of liver tumor in CT images with deep convolutional neural networks. *J Comput Commun*. (2015) 3:146–51. doi: 10.4236/jcc.2015.311023
79. Sun C, Guo S, Zhang H, Li J, Chen M, Ma S, et al. Automatic segmentation of liver tumors from multiphase contrast-enhanced CT images based on FCNs. *Artif Intell Med*. (2017) 83:58–66. doi: 10.1016/j.artmed.2017.03.008
80. Chlebus G, Schenk A, Moltz JH, van Ginneken B, Hahn HK, Meine H. Automatic liver tumor segmentation in CT with fully convolutional neural networks and object-based postprocessing. *Sci Rep*. (2018) 8:15497. doi: 10.1038/s41598-018-33860-7
81. Chen L, Song H, Wang C, Cui Y, Yang J, Hu X, et al. Liver tumor segmentation in CT volumes using an adversarial densely connected network. *BMC Bioinform*. (2019) 20:1–13. doi: 10.1186/s12859-019-3069-x
82. Chen W-F, Ou H-Y, Liu K-H, Li Z-Y, Liao C-C, Wang S-Y, et al. In-series U-Net network to 3D tumor image reconstruction for liver hepatocellular carcinoma recognition. *Diagnostics*. (2020) 11:11. doi: 10.3390/diagnostics11010011
83. Shi W, Kuang S, Cao S, Hu B, Xie S, Chen S, et al. Deep learning assisted differentiation of hepatocellular carcinoma from focal liver lesions: choice of four-phase and three-phase CT imaging protocol. *Abdominal Radiol*. (2020) 45:2688–97. doi: 10.1007/s00261-020-02485-8
84. Vivian R, Szeksin A, Lev-Cohain N, Sosna J, Joskowicz L. Automatic detection of new tumors and tumor burden evaluation in longitudinal liver CT scan studies. *Int J Comput Assist Radiol Surg*. (2017) 12:1945–57. doi: 10.1007/s11548-017-1660-z
85. Jansen MJ, Kuijf HJ, Veldhuis WB, Wessels FJ, Viergever MA, Pluim JP. Automatic classification of focal liver lesions based on MRI and risk factors. *PLoS ONE*. (2019) 14:e0217053. doi: 10.1371/journal.pone.0217053
86. Hamm CA, Wang CJ, Savic LJ, Ferrante M, Schobert I, Schlachter T, et al. Deep learning for liver tumor diagnosis part I: development of a convolutional neural network classifier for multi-phasic MRI. *Eur Radiol*. (2019) 29:3338–47. doi: 10.1007/s00330-019-06205-9
87. Oyama A, Hiraoka Y, Obayashi I, Saikawa Y, Furui S, Shiraishi K, et al. Hepatic tumor classification using texture and topology analysis of non-contrast-enhanced three-dimensional T1-weighted MR images with a radiomics approach. *Sci Rep*. (2019) 9:8764. doi: 10.1038/s41598-019-45283-z
88. Trivizakis E, Manikis GC, Nikiforaki K, Drevelegas K, Constantinides M, Drevelegas A, et al. Extending 2-D convolutional neural networks to 3-D for advancing deep learning cancer classification with application to MRI liver tumor differentiation. *IEEE J Biomed Health Inform*. (2018) 23:923–30. doi: 10.1109/JBHI.2018.2886276
89. Kim J, Min JH, Kim SK, Shin S-Y, Lee MW. Detection of hepatocellular carcinoma in contrast-enhanced magnetic resonance imaging using deep learning classifier: a multi-center retrospective study. *Sci Rep*. (2020) 10:9458. doi: 10.1038/s41598-020-65875-4
90. Zhen S, Cheng M, Tao Y, Wang Y, Juengpanich S, Jiang Z, et al. Deep learning for accurate diagnosis of liver tumor based on magnetic resonance imaging and clinical data. *Front Oncol*. (2020) 10:680. doi: 10.3389/fonc.2020.00680
91. Wu Y, White GM, Cornelius T, Gowdar I, Ansari MH, Supanich MP, et al. Deep learning LI-RADS grading system based on contrast enhanced multiphasic MRI for differentiation between LR-3 and LR-4/LR-5 liver tumors. *Ann Transl Med*. (2020) 8:701. doi: 10.21037/atm.2019.12.151
92. Liang W, Shao J, Liu W, Ruan S, Tian W, Zhang X, et al. Differentiating hepatic epithelioid angiomyolipoma from hepatocellular carcinoma and focal nodular hyperplasia via radiomics models. *Front Oncol*. (2020) 10:564307. doi: 10.3389/fonc.2020.564307
93. Bousabarah K, Letzen B, Tefera J, Savic L, Schobert I, Schlachter T, et al. Automated detection and delineation of hepatocellular carcinoma on multiphasic contrast-enhanced MRI using deep learning. *Abdominal Radiol*. (2021) 46:216–25. doi: 10.1007/s00261-020-02604-5
94. Oestmann PM, Wang CJ, Savic LJ, Hamm CA, Stark S, Schobert I, et al. Deep learning-assisted differentiation of pathologically proven atypical and typical hepatocellular carcinoma (HCC) versus non-HCC on contrast-enhanced MRI of the liver. *Eur Radiol*. (2021) 31:4981–90. doi: 10.1007/s00330-020-07559-1